Bioorganic & Medicinal Chemistry Letters 29 (2019) 1370–1374

Contents lists available at ScienceDirect

Bioorganic & Medicinal Chemistry Letters

journal homepage: www.elsevier.com/locate/bmcl

Ultra-potent vinblastine analogues improve on-target activity of the parent microtubulin-targeting compound

Aleksandar Radakovic, Dale L. Boger*

Department of Chemistry and Skaggs Institute of Chemical Biology, The Scripps Research Institute, 10550 N. Torrey Pines Road, La Jolla, CA 92037, USA

ARTICLE INFO

Keywords:
Vinblastine
Vinca alkaloids
Vinblastine analogues
Tubulin
Microtubulin

ABSTRACT

In recent efforts, several C20′ urea vinblastine analogues were discovered that displayed remarkable potency against vinblastine-sensitive tumor cell lines (IC_{50} 50–75 pM), being roughly 100-fold more potent than vinblastine, and that exhibited decreased susceptibility to Pgp efflux-derived resistance in a vinblastine-resistant cell line. Their extraordinary activity indicate that it is not likely or even possible that their cellular functional activity is derived from stoichiometric occupancy of the intracellular tubulin binding sites. Rather, their potency indicates sub-stoichiometric or even catalytic occupancy of candidate binding sites may be sufficient to disrupt tubulin dynamics or microtubule assembly during mitosis. We detail efforts to delineate the underlying behavior responsible for the increased potency and show that the ultra-potent extended C20′ ureas retain the mechanistic behavior of vinblastine, display enhanced affinity for tubulin and on-target activity approximately 100-fold both in vitro and in HeLa cells, but do not show evidence of catalytic disassembly of microtubulin. We also use the analogues to show that, in live interphase cells, the effects of the vinblastine class of drugs do not display a catastrophic effect on the microtubule skeleton, but rather a subtler insult to its dynamicity, acting as sub-stoichiometric drugs that inhibit normal microtubulin maturation and dynamics.

The Vinca alkaloids belong to the group of microtubule-targeting agents and represent an important class of chemotherapeutics used in the clinic to treat a variety of cancers.[1–3] Their underlying mechanism of action involves binding with tubulin and disruption of microtubule formation that is essential to the proper functioning of the cell cytoskeleton, intracellular transport, mitosis, apoptosis, cell migration, and many other vital mechanisms within the cell.[4–6] The disruption of microtubules and their dynamic behavior by microtubule-targeting agents has been shown to be the chief mechanism behind their efficacy in suppressing growth of rapidly-dividing cells. Microtubule-targeting agents have been traditionally classified as either microtubule-stabilizing or microtubule-destabilizing agents.[7,8] One of the most extensively studied microtubulin-destabilizing agents, vinblastine (**1**, Figure 1), is used in the clinic in highly successful combination therapies to treat Hodgkin's disease, testicular cancer, ovarian cancer, breast cancer, head and neck cancer, Kaposi sarcoma, and non-Hodgkin's lymphoma.[9] However, a major limitation to its clinical efficacy has been the acquired resistance mediated by the increased expression of the P-glycoprotein (Pgp) efflux pump.[10]

Due to recent advances in the total synthesis of vinblastine, a large number of analogues exploiting strategic changes in the upper catharanthine subunit have been synthesized, evaluated, and disclosed in our efforts.[11–24] Among them, several C20′ urea vinblastine analogues (**2, 3, 4**) displayed remarkable potency against vinblastine-sensitive cell lines (IC_{50} 50–75 pM; L1210, HCT116) and decreased susceptibility to Pgp efflux-derived resistance in the vinblastine-resistant cell line HCT116/VM46 (Figure 2).[23] The extended C20′ ureas of these analogues continue to bind along and further disrupt the protein–protein interaction at the tubulin α/β head-to-tail dimer–dimer interface. Although the structure of the ultra-potent C20′ ureas may appear unusual on first inspection, they represent rational structural additions with appropriate conformational constraints to a specific site on the natural product to further enhance disruption of the target protein–protein interaction. The three ultra-potent vinblastines **2–4**, each 100-fold more potent than vinblastine, displayed a much stronger binding affinity for tubulin than vinblastine, 10′-fluorovinblastine (**5**, 10-fold more potent than vinblastine),[16] and other less potent C20′ ureas or amides.[20–24] Although it is not possible to rule out the impact of other features or potentially an unrecognized second mechanism of action, the direct correlation of functional cell growth inhibition activity with tubulin binding affinity and the relative magnitude of the effects suggested that the properties of the potent and ultra-potent C20′ ureas are derived predominately, if not exclusively, from on-target effects on tubulin. Moreover, the extraordinary activity of the ultra-potent analogues indicate that it is not

* Corresponding author.
E-mail address: dale.boger@outlook.com (D.L. Boger).

https://doi.org/10.1016/j.bmcl.2019.03.036
Received 26 February 2019; Received in revised form 21 March 2019; Accepted 25 March 2019
Available online 26 March 2019
0960-894X/

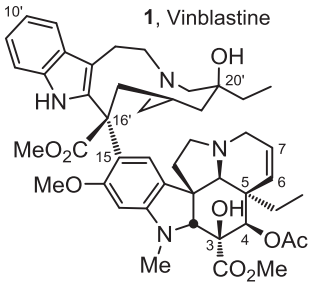

Figure 1. Structure of vinblastine (**1**).

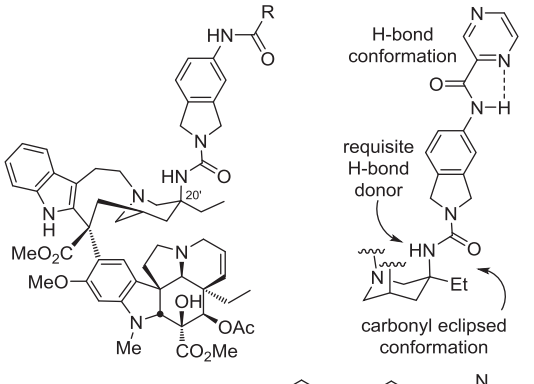

cell line	1, vinblastine	2	3	4
		IC_{50} (nM)		
L1210	6.0	0.059	0.062	0.059
HCT116	6.8	0.075	0.074	0.067
HCT116/VM46	600	0.83	0.88	0.87
HeLa	7.8	0.083	nd	nd

Figure 2. Structure and activity of vinblastine extended C20′ urea analogues. Cell growth inhibition against L1210 (mouse leukemia), HCT116 (human colon cancer) and HCT116/VM46 (matched resistant human colon cancer) tumor cell lines, the latter of which exhibits resistance (ca. 100-fold) to vinblastine through overexpression of P-glycoprotein (Pgp).[23] nd = not determined.

likely or even possible that their cellular functional activity is derived from stoichiometric occupancy of the relatively large total number of intracellular tubulin binding sites. Rather, their potency indicates sub-stoichiometric or even catalytic occupancy of candidate binding sites may be sufficient to disrupt tubulin dynamics or microtubule assembly during mitosis. The question the ultra-potent vinblastines pose is whether sub-stoichiometric binding site occupancy is sufficient to either trap/cap polymerizing microtubulin in non-productive conformations or disrupt microtubulin dynamics like vinblastine, or whether such compounds serve catalytically to actively disassemble microtubulin. Herein, we detail efforts to delineate the underlying behavior responsible for such increased potency. We show that the ultra-potent extended C20′ ureas retain the mechanistic behavior of vinblastine, display enhanced affinity for tubulin in vitro (ca. 100-fold), and exhibit increased on-target activity in mitotic cells (ca 100-fold), but do not show evidence of catalytic disassembly of microtubulin. We also use the analogues to show that, in live interphase cells, the effects of the vinblastine class of drugs do not display a catastrophic effect on the microtubule skeleton, but rather a subtler insult to its dynamicity.

In vitro tubulin binding studies. We have previously shown that the ultra-potent vinblastine extended C20′ ureas (**2**–**4**) bind tubulin with

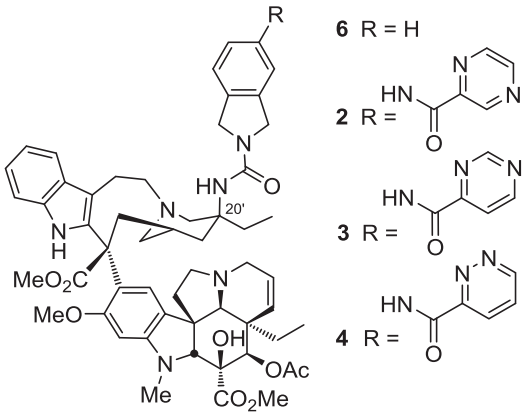

compd	% displacement	IC_{50} (nM, HCT116)
1	31 ± 9%	6.8
6	49 ± 15%	0.6
2	105 ± 5%	0.07
3	104 ± 12%	0.07
4	101 ± 4%	0.07

Figure 3. Tubulin binding affinity. Tubulin (0.1 mg/mL, 0.91 μM) was incubated with BODIPY-vinblastine (BODIPY-VBL) and the vinblastine analogue (1.8 μM) at 37 °C in PEM buffer containing 850 μM GTP and the measured % displacement of BODIPY-VBL is recorded. Reported values are the average 4 measurements ± the standard deviation and have been disclosed elsewhere.[23]

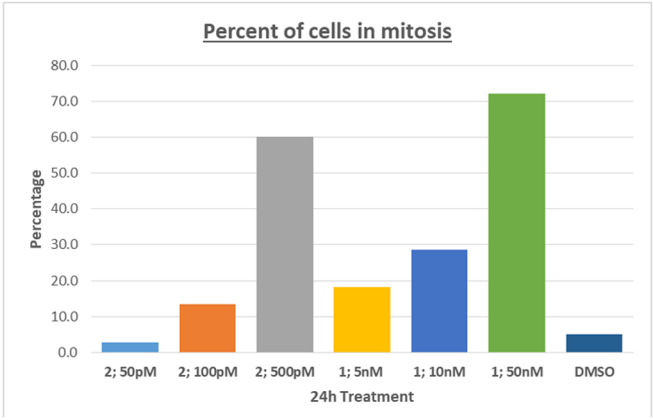

Figure 4. Compounds **1** and **2** cause mitotic block in a concentration-dependent manner (n = 95–208) with **2** being roughly 100-fold more potent than vinblastine (**1**).

much greater affinity than vinblastine or less potent C20′ ureas (e.g., **6**). They displayed pronounced trends correlating directly with cell growth inhibition, displacing 100% of a BODIPY-vinblastine probe in competitive ligand binding studies, indicative of a much increased on-target binding affinity compared to the parent compound (Figure 3).[23] We sought to determine whether this increased binding affinity to tubulin correlated with an observable global effect on microtubules in vitro. First, stable turbid microtubules were prepared by either utilizing GMPCPP, a slowly hydrolysable GTP analogue, or paclitaxel, a known microtubulin-stabilizing agent. Such microtubules were treated with varying concentrations of **2** and **3**. Neither analogue displayed an effect on GMPCPP- or paclitaxel-polymerized microtubules as monitored at

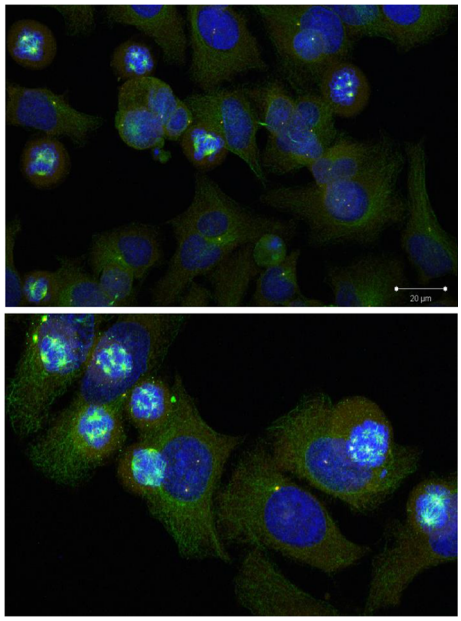

Figure 5. Both **1** and **2** cause the same phenotypic behavior of microtubulin and mitotic spindles in HeLa cells: multiple clumps of microtubules found in arbitrary parts of cells. Top: HeLa cells treated with 10 nM vinblastine for 20 h. Bottom: HeLa cells treated with 500 pM **2** for 20 h. Bar = 20 µm. Blue = nuclei, green = beta-tubulin, red = gamma-tubulin. A normal single mitotic spindle in the nucleus can been seen in bottom left corner of top panel or bottom right corner of bottom panel. (For interpretation of the references to colour in this figure legend, the reader is referred to the web version of this article.)

350 nm for microtubulin depolymerization (Supporting Information Figure S1). Significantly, neither compound displayed evidence of active, catalytic depolymerization of microtubulin in this assay. Additionally and although the assay is known to be insensitive and largely non-predictive, the analogues **2–4** displayed no effect on microtubule polymerization in the commercially available Chemicon In Vitro Tubulin Polymerization Assay Kit at pM and nM concentrations (Supporting Information Figure S2). However, **2** mirrored the effect of vinblastine on microtubule polymerization at µM concentrations where polymerization was significantly inhibited and delayed (Supporting Information Figure S3).

Fixed-cell immunofluorescence. To establish whether the ultra-potent extended C20′ ureas display their exceptional potency due to a catastrophic effect on the global microtubule skeleton, HeLa cells were treated with a low, sub-stoichiometric dose of **2** for 20 h and their microtubule skeletons visualized with fluorescence microscopy in fixed, permeabilized cells treated with primary antibodies followed by secondary fluorescent antibodies for visualization of beta- and gamma-tubulin and Hoecsht dye for nuclear staining. Due to the structural and functional similarity of **2–4**, only **2** was used in these and subsequent studies. The actin skeleton was also visualized by rhodamine–phalloidin staining. No significant effect on the global skeleton was observed, including no catastrophic deficiencies that would be characteristic of active catalytic microtubulin depolymerization (Supporting Information Figure S4). A range of concentrations of **1** and **2** were used to assess their ability to cause mitotic block, a mechanism of action observed with vinblastine in rapidly-dividing cells.[25] Both compounds displayed a concentration-dependent capacity to cause mitotic block as measured by the proportion of mitotic cells within the cell populations, with analogue **2** causing roughly the same proportion of cells to be blocked in mitosis at 100-fold lower concentrations than **1** (Figure 4). This observation is consistent with and quantitatively correlates with the functional cell growth inhibition assays in which **2** displays approximately a 100-fold lower IC_{50} than **1** (Figure 2).

To further corroborate that the new analogues mirror the mechanism of vinblastine, we focused on small populations of cells affected by the compounds and assessed the disposition of their microtubules. Both **1** and **2** caused numerous multiple clumps of tubulin within a single cell, in addition to what should be a single mitotic spindle, which occurred in arbitrary parts of cells (Figure 5). Some clumps could be characterized as partial spindles due to their clear attachment to condensed chromosome. However, other observed clumps of tubulin lack centrosomes and indicate that the compounds promote tubulin nucleation without the need for microtubulin organizing centers (mTOCs). The individual antibody labeling also indicated the compounds (**1** and **2**) affect the alpha and beta, but not gamma, tubulin isoforms (Supporting Information Figure S5).

Live-cell fluorescence. After assessing the microtubule disposition post drug treatment, we sought to identify the mechanism by which these compounds disrupt the microtubules in real time. HeLa cells were transiently transfected with GFP-tubulin, treated with **2** for 5 h, and their microtubules monitored using either LSM 780 confocal or TIRF Nikon microscopy. Deconvolution of data followed by object reconstruction in Imaris allowed us to track the proportion of long (> 3 µm), medium ($1 < x < 3$ µm), or short (< 1 µm) microtubules frame by frame (TIRF, Figure 6). This approach enabled us to unbiasedly monitor the dynamics of the microtubules on a global level in multiple cells. Although no quantitative method was designed to represent the change in dynamicity, it is clear from the qualitative data that **2** suppresses the number of microtubules changing between the outlined categories, which can be directly correlated with a suppression of the dynamic nature of microtubules by **2** (Figure 6). It also appears that **2** substantially increased the ratio of short versus medium and long microtubules compared to control consistent with a role in inhibiting microtubulin maturation. These studies suggest that **2** and related ultra-potent vinblastine analogues are not acting as catalysts actively promoting microtubulin depolymerization, but rather as sub-stoichiometric drugs that inhibit microtubulin maturation and dynamics.

The ultra-potent vinblastine analogues studied herein underscore the opportunities of performing medicinal chemistry optimization even on established complex natural products to produce molecules with improved capabilities. Not only do **2–4** largely overcome the Pgp-mediated resistance observed with vinblastine, but they substantially improve both the on-target affinity and functional activity of the parent molecule nearly 100-fold. These molecules represent an example where increasing the complexity of an already complex molecule can add multiple beneficial features. The added urea at C20′ inhibits the molecules' capabilities to serve as a substrate for Pgp efflux while simultaneously increasing the on-target tubulin binding affinity, where the rigid extended urea further disrupts the α/β tubulin dimer–dimer interface.[24] In earlier studies, these analogues were also shown to be unaffected by the overexpression of type III ß-tubulin, another known mechanism of resistance to other microtubulin targeting agents, highlighting their potential for treating disease that is refractory to other drugs (e.g., taxol).[26–28] Herein, we show that that the ultra-potent analogues **2–4** display a mechanism of action analogous to vinblastine itself, just at concentrations approximately 100-fold lower than vinblastine. This behavior is clearly sub-stoichiometric relative to available target sites in the cell, is unlikely to involve an unrecognized second mechanism of action not observed with vinblastine itself, and does not appear to be catalytic in its functional behavior.

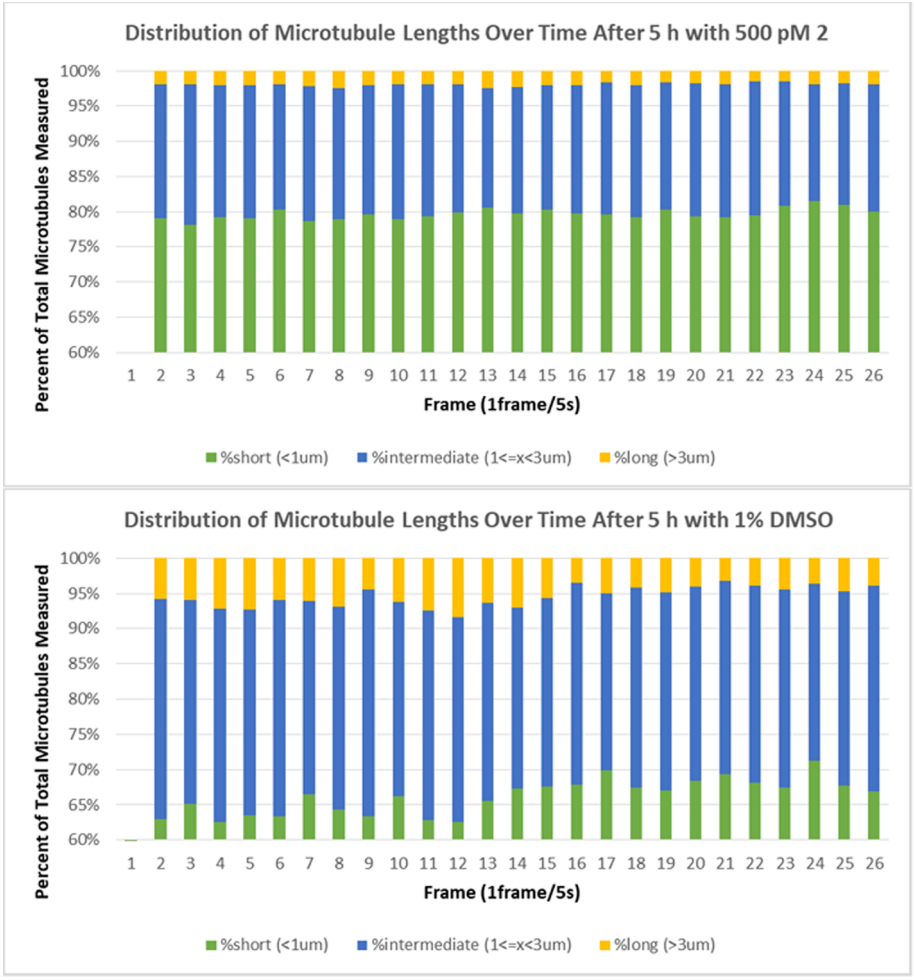

Figure 6. Monitoring microtubule state and dynamics in real time in live HeLa cells with and without treatment with **2** (500 pM).

Acknowledgements

We gratefully acknowledge the financial support of the National Institutes of Health (CA042056, D.L.B.) and the Skaggs Institute for Chemical Biology. We also acknowledge and thank William B. Kiosess, PhD, and Kersi Prestonjamasp, PhD, for their advice and helpful discussion regarding the technical and analytical microscopy details.

Appendix A. Supplementary data

Supplementary data to this article can be found online at https://doi.org/10.1016/j.bmcl.2019.03.036.

References

1. Neuss N, Neuss MN. Therapeutic use of bisindole alkaloids from catharanthus. In: The Alkaloids; Brossi A, Suffness M, Eds. Academic: San Diego, CA, 1990;37:229 – 240.
2. Pearce HL. Medicinal chemistry of bisindole alkaloids from catharanthus. In The Alkaloids; Brossi A, Suffness M, Eds. Academic: San Diego, CA, 1990;37:145 – 204.
3. Kuehne ME, Marko I. Syntheses of vinblastine-type alkaloids. In The Alkaloids; Brossi A, Suffness M, Eds. Academic: San Diego, CA, 1990;37:77 – 132.
4. Jordan MA, Wilson L. Microtubules as a target for anticancer drugs. *Nat Rev Cancer.* 2004;4:253–265.
5. S.. Microtubules in cell migration. *Annu Rev Cell Dev Biol.* 2013;29:471–499.
6. Nogales E. Structural insights into microtubule function. *Annu Rev Biochem.* 2000;69:277–302.
7. Steinmetz MO, Prota AE. Microtubule-targeting agents: strategies to hijack the cytoskeleton. *Trends Cell Biol.* 2018;28:776–792.
8. Jordan MA, Thrower D, Wilson L. Mechanism of inhibition of cell proliferation by Vinca alkaloids. *Cancer Res.* 1991;51:2212–2222.
9. National Cancer Institute. Vinblastine sulfate: use in cancer. Posted 2011; Updated 2014; Accessed 2018.
10. Persidis A. Cancer multidrug resistance. *Nat Biotechnol.* 1999;17:94–95.
11. (a) Ishikawa H, Colby DA, Boger DL. Direct coupling of catharanthine and vindoline to provide vinblastine: total synthesis of (+)- and ent-(–)-vinblastine. *J Am Chem Soc.* 2008;130:420–421;

    (b) Ishikawa H, Colby DA, Seto S, et al. Total synthesis of vinblastine, vincristine, related natural products, and key structural analogues. *J Am Chem Soc.* 2009;131:4904–4916;

    (c) Gotoh H, Sears JE, Eschenmoser A, Boger DL. New insights into the mechanism and an expanded scope of the Fe(III)-mediated vinblastine coupling reaction. *J Am Chem Soc.* 2012;134:13240–13243.
12. (a) Sears JE, Boger DL. Total synthesis of vinblastine, related natural products, key analogues and development of inspired methodology suitable for the systematic study of their structure–function properties. *Acc Chem Res.* 2015;48:653–662;

    (b) Boger DL. The difference a single atom can make: synthesis and design at the chemistry – biology interface. *J Org Chem.* 2017;82:11961–11980.
13. (a) Ishikawa H, Elliott GI, Velcicky J, Choi Y, Boger DL. Total synthesis of (–)- and ent-(+)-vindoline and related alkaloids. *J Am Chem Soc.* 2006;128:10596–10612;

    (b) Choi Y, Ishikawa H, Velcicky J, Elliott GI, Miller MM, Boger DL. Total synthesis of (–)- and ent-(+)-vindoline. *Org Lett.* 2005;7:4539–4542;

    (c) Sears JE, Barker TJ, Boger DL. Total synthesis of (–)-vindoline and (+)-4-epi-vindoline based on a 1,3,4-oxadiazole tandem intramolecular [4+2]/[3+2] cycloaddition cascade initiated by an allene dienophile. *Org Lett.* 2015;17:5460–5463;

    (d) Sasaki Y, Kato D, Boger DL. Asymmetric total synthesis of vindorosine, vindoline, and key vinblastine analogues. *J Am Chem Soc.* 2010;132:13533–13544;

    (e) Kato D, Sasaki Y, Boger DL. Asymmetric total synthesis of vindoline. *J Am Chem Soc.* 2010;132:3685–3687;

    (f) Wilkie GD, Elliott GI, Blagg BSJ, et al. Intramolecular Diels-Alder and tandem intramolecular Diels–Alder/1,3-dipolar cycloaddition reactions of 1,3,4-oxadiazoles.

J Am Chem Soc. 2002;124:11292–11294;

(g) Elliott GI, Fuchs JR, Blagg BSJ, et al. Intramolecular Diels–Alder/1,3-dipolar cycloaddition cascade of 1,3,4-oxadiazoles. *J Am Chem Soc.* 2006;128:10589–10595.

14. Va P, Campbell EL, Robertson WM, Boger DL. Total synthesis and evaluation of a key series of C5-substituted vinblastine derivatives. *J Am Chem Soc.* 2010;132:8489–8495.
15. Tam A, Gotoh H, Robertson WM, Boger DL. Catharanthine C16 substituent effects on the biomimetic coupling with vindoline: preparation and evaluation of a key series of vinblastine analogues. *Bioorg Med Chem Lett.* 2010;20:6408–6410.
16. Gotoh H, Duncan KK, Robertson WM, Boger DL. 10'-Fluorovinblastine and 10'-fluorovincristine: synthesis of a key series of modified vinca alkaloids. *ACS Med Chem Lett.* 2011;2:948–952.
17. (a) Schleicher KD, Sasaki Y, Tam A, Kato D, Duncan KK, Boger DL. Total synthesis and evaluation of vinblastine analogues containing systematic deep-seated modifications in the vindoline subunit ring system: core redesign. *J Med Chem.* 2013;56:483–495;

(b) Campbell EL, Skepper CK, Sankar K, Duncan KK, Boger DL. Transannular Diels-Alder/1,3-dipolar cycloaddition cascade of 1,3,4-oxadiazoles: total synthesis of a unique set of vinblastine analogues. *Org Lett.* 2013;15:5306–5309.

18. Yang S, Sankar K, Skepper CK, et al. Total synthesis of a key series of vinblastines modified at C4 that define the importance and surprising trends in activity. *Chem Sci.* 2017;8:1560–1569.
19. (a) Allemann O, Brütsch MM, Lukesh III JC, Brody DM, Boger DL. Synthesis of a potent vinblastine: rationally designed added benign complexity. *J Am Chem Soc.* 2016;138:8376–8379;

(b) Allemann O, Cross RM, Brütsch MM, Radakovic A, Boger DL. Key analogs of a uniquely potent synthetic vinblastine that contain modifications of the C20' ethyl substituent. *Bioorg Med Chem Lett.* 2017;27:3055–3059.

20. (a) Leggans EK, Barker TJ, Duncan KK, Boger DL. Iron(III)/$NaBH_4$-mediated additions to unactivated alkenes: synthesis of novel C20' vinblastine analogues. *Org Lett.* 2012;14:1428–1431;

(b) Barker TJ, Boger DL. Fe(III)/$NaBH_4$-mediated free radical hydrofluorination of unactivated alkenes. *J Am Chem Soc.* 2012;134:13588–13591.

21. Leggans EK, Duncan KK, Barker TJ, Schleicher KD, Boger DL. A remarkable series of vinblastine analogues displaying enhanced activity and an unprecedented tubulin binding steric tolerance: C20' urea derivatives. *J Med Chem.* 2013;56:628–639.
22. Barker TJ, Duncan KK, Otrubova K, Boger DL. Potent vinblastine C20' ureas displaying additionally improved activity against a vinblastine-resistant cancer cell line. *ACS Med Chem Lett.* 2013;4:985–988.
23. Carney DW, Lukesh III JC, Brody DM, Brutsch MM, Boger DL. Ultrapotent vinblastines in which added molecular complexity further disrupts the target tubulin dimer – dimer interface. *Proc Natl Acad Sci USA.* 2016;113:9691–9698.
24. Lukesh III JC, Carney DW, Dong H, et al. Vinblastine 20' amides: synthetic analogues that maintain or improve potency and simultaneously overcome Pgp-derived efflux resistance. *J Med Chem.* 2017;60:7591–7604.
25. Wendell KL, Wilson L, Jordan MA. Mitotic block in HeLa cells by vinblastine: ultrastructural changes in kinetochore – microtubule attachment and in centrosomes. *J Cell Sci.* 1993;104:261–274.
26. Radakovic A, Boger DL. High expression of class III β-tubulin has no impact on functional cancer cell growth inhibition of a series of key vinblastine analogs. *Bioorg Med Chem Lett.* 2018;28:853–865.
27. Sève P, Dumontet C. Is class III beta-tubulin a predictive factor in patients receiving tubulin-binding agents? *Lancet Oncol.* 2008;9:168–175.
28. Kavallaris M, Kuo DY, Burkhart CA, et al. Taxol-resistant epithelial ovarian tumors are associated with altered expression of specific beta-tubulin isotypes. *J Clin Invest.* 1997;100:1282–1293.